J Biomol NMR (2007) 39:63–72
DOI 10.1007/s10858-007-9176-4

ARTICLE

Positioning of the Alzheimer Aβ(1–40) peptide in SDS micelles using NMR and paramagnetic probes

Jüri Jarvet · Jens Danielsson · Peter Damberg · Marta Oleszczuk · Astrid Gräslund

Received: 26 April 2007 / Accepted: 19 June 2007 / Published online: 27 July 2007

Abstract NMR spectroscopy combined with paramagnetic relaxation agents was used to study the positioning of the 40-residue Alzheimer Amyloid β-peptide Aβ(1–40) in SDS micelles. 5-Doxyl stearic acid incorporated into the micelle or Mn^{2+} ions in the aqueous solvent were used to determine the position of the peptide relative to the micelle geometry. In SDS solvent, the two α-helices induced in Aβ(1–40), comprising residues 15–24, and 29–35, respectively, are surrounded by flexible unstructured regions. NMR signals from these unstructured regions are strongly attenuated in the presence of Mn^{2+} showing that these regions are positioned mostly outside the micelle. The central helix (residues 15–24) is significantly affected by 5-doxyl stearic acid however somewhat less for residues 16, 20, 22 and 23. This α-helix therefore resides in the SDS headgroup region with the face with residues 16, 20, 22 and 23 directed away from the hydrophobic interior of the micelle. The C-terminal helix is protected both from 5-doxyl stearic acid and Mn^{2+}, and should be buried in the hydrophobic interior of the micelle. The SDS micelles were characterized by diffusion and ^{15}N-relaxation measurements. Comparison of experimentally determined translational diffusion coefficients for SDS and Aβ(1–40) show that the size of SDS micelle is not significantly changed by interaction with Aβ(1–40).

Keywords NMR · Amyloid β-peptide · SDS micelle

Introduction

In the Alzheimer's disease, senile plaques are found in the extra cellular compartment in the brain. The Alzheimer amyloid β-peptide (Aβ) is the major component of the amyloid plaques of the brains of patients suffering from the Alzheimer's disease. The Aβ-peptide is a 39–42-residue peptide proteolytically cleaved from much larger proteins known as Amyloid Precursor Proteins (APPs), which consist of 695–770 amino acids with a single hydrophobic transmembrane region. The leading theory explaining the disease progress has been the Amyloid cascade hypothesis, which includes aggregation of the Alzheimer Aβ peptide and the formation of the fibrils which compose plaques (Hardy and Selkoe 2002; Selkoe 2003; Chiti and Dobson 2006). More recently, an alternative version of the amyloid cascade hypothesis suggests that the induced memory loss and neuronal death are based on the impact of soluble oligomers of Aβ (Hardy and Selkoe 2002; Chiti and Dobson 2006; Klein et al. 2001). A stable and toxic oligomeric species has recently been found (Lesné et al. 2006; Barghorn et al. 2005), and this oligomer consists of 12 peptides. The oligomer has a protease protected hydrophobic core consisting of the C-terminal region of the peptide (Barghorn et al. 2005). The soluble oligomeric Aβ shows common structural features with other soluble oligomeric amyloid peptides, such as α-synuclein, IAPP, poly (Q) and prion fragment (106–126) (Kayed et al. 2003, 2004).

The toxic mechanism of the oligomers is not known in detail but increasing evidence suggests that membrane interaction plays an important part in neurotoxicity. Aβ

Electronic supplementary material The online version of this article (doi:10.1007/s10858-007-9176-4) contains supplementary material, which is available to authorized users.

J. Jarvet (✉) · J. Danielsson · P. Damberg · M. Oleszczuk · A. Gräslund
Department of Biochemistry and Biophysics, Arrhenius Laboratories, Stockholm University, Stockholm 106 91, Sweden
e-mail: jyri.jarvet@dbb.su.se

oligomers penetrate and insert into lipid membranes, while monomers are less membrane active (Curtain et al. 2001; Ashley et al. 2006; Sokolov et al. 2006; Lee et al. 1995). Membrane composition is important for Aβ oligomer insertion. Aβ oligomers insert into membranes containing at least 30% cholesterol and form channels and thereby compromise membrane integrity (Ashley et al. 2006; Ji et al. 2002; Micelli et al. 2004). However, cholesterol seems to inhibit insertion of the hydrophobic fragment Aβ (25–35). Aβ has also been studied in association with charged and neutral lipid monolayers and bilayers (Bokvist et al. 2004; Ambroggio et al. 2005) and Aβ seems to more easily interact with negatively charged lipids than with neutral lipids. Terzi et al. found Aβ(1–40) to insert only into very loosely packed monolayers (Terzi et al. 1994; Ege and Lee 2004). Also other studies have shown that compressibility and surface pressure of the membrane strongly affects Aβ membrane insertion (Sokolov et al. 2006; Lee et al. 1995).

In the membrane the oligomers have been suggested to form cation conducting pores/channels that result in an increase in intra-cellular calcium levels (Arispe 2004; Quist et al. 2005; Alarcón et al. 2006; Demuro et al. 2005). This has been suggested as a possible toxic mechanism of Aβ. The existence of Aβ channels has been both predicted theoretically (Durell et al. 1994) and studied experimentally using patch clamp techniques as well as AFM and EPR (Lin et al. 2001; Curtain et al. 2001). The theoretical work suggested a channel that consists of 6 subunits with a C-terminal α-helix buried into the membrane, a central α-helix located on the lipid/solvent interface and the hydrophilic N-terminus pointing into the channel (Durell et al. 1994). The peptide undergoes a structural change from predominantly β-strand when the peptide is located at the lipid surface to a high fraction of α-helix in the inserted form (58%) (Ji et al. 2002), also in agreement with α-helices as an important structural motif in the Aβ channel. The oligomers have been shown to bind specifically to the synaptic regions of the neuron (Lacor et al. 2004; Barghorn et al. 2005).

The present study concerns the positioning of the monomeric Aβ peptide in a lipid-mimicking environment. Several previous structural studies of the Aβ peptide in lipid-mimicking environments have been reported, all pointing towards the presence of two α-helical regions connected by a more flexible and disordered link. In organic solvents such as aqueous trifluoroethanol (TFE) or hexafluoroisopropanol (HFiP) and at low pH, the structure has been reported as α-helical for residues 15–23 and 31–35 (Sticht et al. 1995; Crescenzi et al. 2002). Crescenzi et al. found the peptide to be boomerang shaped and presented a hypothetical structure where the second, C-terminal helix is inserted into the membrane, and the remaining part of the peptide positioned at the membrane surface.

SDS detergent micelles provide a better system than the organic solvents for modeling the interaction between the peptide and a phospholipid bilayer. The small size of the micelles allows good spectral resolution in NMR. In lithium or sodium dodecyl sulphate (LiDS or SDS) micelles at pH below 5, the shorter fragments 12–28, 25–35 and 1–28 all form α-helical structures (Talafous et al. 1994; Kohno et al. 1996; Fletcher and Keire 1997). Based on amide proton exchange data, Aβ(25–35) was claimed to insert itself into the interior of the micelle, while Aβ(1–28) is positioned at the micelle surface.

For the full-length Aβ(1–40) peptide, in SDS solvent and at pH 5.1, α-helical structure is formed within residues 15–24 and 28–36, with a kink or hinge around residues 25–27. The peptide has a bent shape, and was proposed to be partly inserted into the micelle (Coles et al. 1998). At pH 7.2 and in the presence of 15% HFiP, the α-helical regions extend to residues 10–24 and 28–40, and the whole peptide is suggested to reside at the surface of the SDS micelle, without any insertion (Shao et al. 1999). The conformational behavior of Aβ in association with different lipid systems is clearly dependent on experimental conditions such as temperature, solvent and pH. In a study by Curtain et al. only the N-terminus part of Aβ in SDS micelles was shown to be exposed to paramagnetic relaxation enhancement effects by Cu^{2+} suggesting that both the central and C-terminal regions of the peptide are buried into the micelle (Curtain et al. 2001). On the other hand, in cholesterol-containing DMPC vesicles the C-terminal region is protected from proteolytic cleavage while the central and N-terminal regions are not. Also, in the vesicles 58% of the peptide is estimated to adopt an α-helical conformation. This suggests that the C-terminal α-helix is buried into the lipid of the vesicle while the central helix resides on the vesicle surface (Ji et al. 2002).

Whereas structure induction in Aβ by membrane mimicking solvents seems to be agreed on, the positioning of the Aβ peptide relative to membrane surface is still questionable. In the study by Coles et al. (1998) the positioning of Aβ in SDS was discussed with respect to the membrane spanning segment of the Amyloid Precursor Protein. Among the three positioning alternatives a preferred hypothetic position had the C-terminal helix of Aβ(1–40) as a membrane inserted region. This discussion inspired the present study. Knowledge about this positioning may provide information on the preferred positioning of Aβ in biological membranes and may give insight into the structural properties of membrane bound oligomeric channels. In the present study we have probed the positioning of Aβ(1–40) in SDS micelles using paramagnetic 5-doxyl fatty acids and Mn^{2+} ions. Reassignment of the

^{13}C, ^{15}N-labelled peptide turned out to be necessary due to conflicting previous reports on assignment (Shao et al. 1999; Mandal et al. 2006). In addition we have carefully characterized the hydrodynamic properties and size of the peptide/SDS complex using NMR diffusion methods.

Materials and methods

The full-length amyloid β-peptide Aβ(1–40) was studied. The unlabeled peptide was purchased from Neosystems, France and Sigma Chemical Co, USA and was used without further purification. ^{15}N-labeled and double ^{13}C,^{15}N-labeled Aβ(1–40) was purchased from rPeptide, USA. For NMR, deuterated SDS-d_{25} from Cambridge Isotope laboratories, USA was used. 5-doxyl-stearic acid was from Sigma, methanol-d_4 for dissolving the stearic acids was purchased from Merck. Peptides were stored frozen and thawed before use. To remove aggregation seeds in the sample, preconditioning of peptide material was carried out by dissolving it in HFiP, followed by freezing on dry ice and lyophilizing. All experiments were performed in 10–20 mM sodium phosphate buffer at pH 7–7.6 at low peptide concentrations (<300 μM) to avoid aggregation. For experiments with 5-doxyl stearic acids 10 mM stock solution of paramagnetic agent dissolved in methanol-d_4 was used. The proper amount was pipeted to the eppendorf tube, dried with nitrogen gas and then the peptide sample was added.

The peptides were dissolved in 10 mM NaOH and sonicated for 1.5 min, after which the buffer was added. Peptide concentrations were 50–300 μM for NMR experiments in 100 mM SDS solution, with 20 mM sodium phosphate buffer in 10% D_2O. All concentrations were determined by weight and the pH was measured using a standard pH-meter equipped with a CMAW711/3.7/180 electrode (Thermo Scientific, UK) directly in the NMR tube.

NMR spectra were acquired using Varian Unity Inova spectrometers operating at 600 and 800 MHz proton resonance frequency. 2D ^1H TOCSY spectra were recorded using 50 ms mixing time. 2D ^1H–^{15}N HSQC spectra were recorded using 79 ms acquisition time in the ^1H dimension and 51 ms acquisition time in the ^{15}N dimension. TROSY spectra were recorded using 102 ms acquisition time and 992 increments in 2.5 kHz window in ^{15}N dimension. 3D HNCA and HNCOCA experiments were acquired at 600 MHz using proton carrier at 4.753 ppm in 8 kHz window, ^{13}C centered at 55.9 ppm in 4.5 kHz window and 128 increments, ^{15}N centered at 118 ppm in 1.5 kHz window using 64 increments. During the carbon evolution time the carbonyl carbons and the β-carbons resonating below 39 ppm were decoupled by adiabatic WURST decoupling (Kupče and Freeman 1995). The spectra were calibrated using the ratio $^{13}C/^1H = 0.25144953$ for carbon and $^{15}N/^1H = 0.101329118$ for nitrogen. Secondary shifts were analyzed relative to random coil values and interpreted as suggested by Wishart et al. (1995).

^{15}N relaxation experiments were performed using a Varian BioPack standard pulse sequence gNhsqc with 2048×96 increments, 32 scans and the transmitter offset placed on the water resonance frequency. The T_1 relaxation experiments were done using 7 relaxation delay times, ranging from 0 to 400 ms. All NMR spectra were processed in Varian vnmr software. Relaxation data, i.e. the maximum peak intensity, was fitted to a single exponential decay using gnuplot 3.7 software.

NMR diffusion measurements were performed with the pulsed field gradient spin-echo experiment (PFG-LED) (Gibbs et al. 1991) in 5 mm NMR tubes. A 600 MHz Varian Inova spectrometer equipped with a HCX probe with z-axis gradient was used for all experiments. To correct for systematic errors due to nonlinearity of the gradient field, a distribution function for the gradient strength was used when calculating the diffusion coefficient (Damberg et al. 2001a). This function was calibrated using a standard sample of 99.95% D_2O. The diffusion experiments were performed using 16 different linearly spaced strengths of gradients with 150 ms longitudinal storage time. Diffusion experiments were done at 25°C.

In order to determine the SDS micelle translational diffusion constant at infinite dilution the concentration dependence of SDS diffusion was studied. On the diffusion time scale, when using NMR to measure diffusion, the chemical exchange of SDS between bound to a micelle and free monomeric SDS is fast and thus the observed diffusion coefficient is the weighted mean of the bound, D_m, and free, D_f, form:

$$D_{\text{obs}} = D_m f_m + D_f f_f \tag{1}$$

where $f_m = (C_{\text{tot}} - C_f)/C_{\text{tot}}$ and $f_f = C_f/C_{\text{tot}}$ is the fraction of SDS molecules, free in solution and bound in micelles respectively. For our purpose, D_m has to be determined in order to make a proper comparison with the peptide/SDS complex, studied via peptide diffusion.

For micelles with no monomeric SDS contribution the concentration dependence of the diffusion coefficient is linear because of obstruction factors. The concentration dependence of the measured diffusion D_m of the micelle is approximately given by:

$$D_m = {}^0D_m\,(1 - 3.2\lambda\Phi) \tag{2}$$

Here ${}^0D_m$ is the SDS micelle diffusion coefficient at infinite dilution, λ is a shape and interaction dependent parameter ($\lambda = 1$ for a hard, non-interacting sphere) and Φ

is the dry volume fraction (Tokuyama and Oppenheim 1994). The SDS monomer diffusion is also related to the volume fraction of SDS by the obstruction exhibited by the micelles on the monomers. This obstruction effect is given by:

$$D_f = {}^0D_f/(1 + \Phi/2) \quad (3)$$

Here ${}^0D_f$ is the monomeric free self diffusion at infinite dilution (Johannesson and Halle 1996). To handle the critical micelle concentration, CMC, the approach suggested by Bax and coworkers was used (Chou et al. 2004): the CMC is approximated as an infinitely sharp transition and it is assumed that for concentrations below CMC no micelles are formed and thus $C_f = C_{tot}$ and $f_f = 1$. For concentrations above CMC C_f = CMC.

Results

The Aβ(1–40) peptide in complex with SDS detergent micelles was investigated by high resolution NMR methods, in order to characterize positioning, secondary structure induction and mobility relative to the micelle, and effect on the hydrodynamic properties of the micelle. In order to clarify previous uncertainties regarding NMR assignment we used a ^{13}C,^{15}N-labeled Aβ(1–40) for a new assignment at our experimental conditions.

NMR assignment

2D and 3D-NMR spectroscopy was used to assign the resonances of Aβ(1–40) in 150 mM SDS environment at 25°C. We had found that spectra recorded at 25°C were of significantly better quality that those recorded at 35°C (data not shown). Figure 1A shows a partial ^{1}H–^{15}N TROSY spectrum in 150 mM d_{25}-SDS at pH 7.4. The spectrum recorded at 800 MHz is well resolved. Only the crosspeaks from the two first N-terminal residues D1 and A2 are missing and all the other residues are resolved. Sequential assignment was achieved using 3D HNCA and HNCOCA experiments (Fig. 1S, Supplementary material). The amide nitrogen, α-proton and α-carbon assignments for Aβ(1–40) in 150 mM SDS solvent at pH 7.4 and 25°C are listed as Supplementary material in Table 1S. We found a number of residue assignments to be significantly different from previous studies under similar conditions (Shao et al. 1999; Mandal et al. 2007).

Figure 2A–C shows the secondary chemical shifts of the α-protons, α-carbons and amide nitrogens of Aβ(1–40) in 150 mM SDS, indicating α-helix induction in the two segments 15–24 and 29–35. In order to further verify the positioning of α-helix regions of the peptide the $d\alpha N(i,i)$/$d\alpha N(i,i+1)$ distance ratios were analyzed. The NOE crosspeak volume ratios were calculated and found to be non-overlapping and reliable for 50% of the residues and shown in Fig. 2E. The position of the two helices determined by the NOE ratio agrees with the positions obtained from the secondary chemical shifts. The secondary chemical shifts obtained from our new assignment and the NOE ratios suggest that the C-terminal helix in SDS is relatively short.

It was proposed by Shao et al. (1999) that a small amount of HFiP (10–15% by volume) in the SDS-water solution does not influence the secondary structure of Aβ(1–40). However, our experiments show that 13% of HFiP has a considerable effect on the chemical shifts of resonances from several Aβ(1–40) residues, as shown in Supplementary material (Fig. 2S and 3S). These residues include several of those that we find buried inside the SDS micelle (see below). Therefore HFiP, which was used as a preconditioning agent for the peptide, was carefully removed from the sample before dissolving it in the SDS micelles.

Positioning of Aβ in the complex with the micelle

The effect of paramagnetic probes was estimated from 2D ^{1}H TOCSY and ^{1}H–^{15}N HSQC experiments or from ^{1}H–^{15}N TROSY experiments by comparing spectra with and without added Mn^{2+} ions or 5-doxyl stearic acid, respectively. Typical Mn^{2+} and 5-doxyl stearic acid concentrations were around 0.1 mM or 2 mM, respectively, selected to produce attenuation by a factor of about 2 for the residues accessible to the paramagnetic probes. TROSY spectra of Aβ(1–40) in SDS at pH 7.3 without and with 5-doxyl stearic acid are shown in Fig. 1A and B. Intensity ratios of remaining amide cross peaks after 5-doxyl stearic acid addition are shown in Fig. 3A. The biggest intensity changes are observed among residues H13–A21. The residues of the central helix (residues 15–24) are overall clearly affected by the 5-doxyl stearic acid. However, the intensity ratios for four residues in this helix, K16, F20, E22, and D23 are relatively high. The helical periodicity indicates that the K16/F20/E22/D23 face of the helix is less accessible than the rest of the helix. The C-terminal α-helix (G29–M35) and further C-terminal residues (V36–V40) are well protected from exposure to the 5-doxyl stearic acid.

The ^{1}H–^{15}N HSQC spectra of Aβ(1–40) in 100 mM SDS at pH 7.4 without and with 0.1 mM Mn^{2+} give another picture (Fig. 1C and D). Figure 3B shows the amide crosspeak intensities along the peptide chain evaluated as fractions remaining after the addition of Mn^{2+} to the SDS solvent. The unstructured regions in both termini as well as the central region, residues 25–28, are all quite strongly affected by the Mn^{2+} ions, whereas the helical regions are on the whole well protected. The protection from Mn^{2+} in

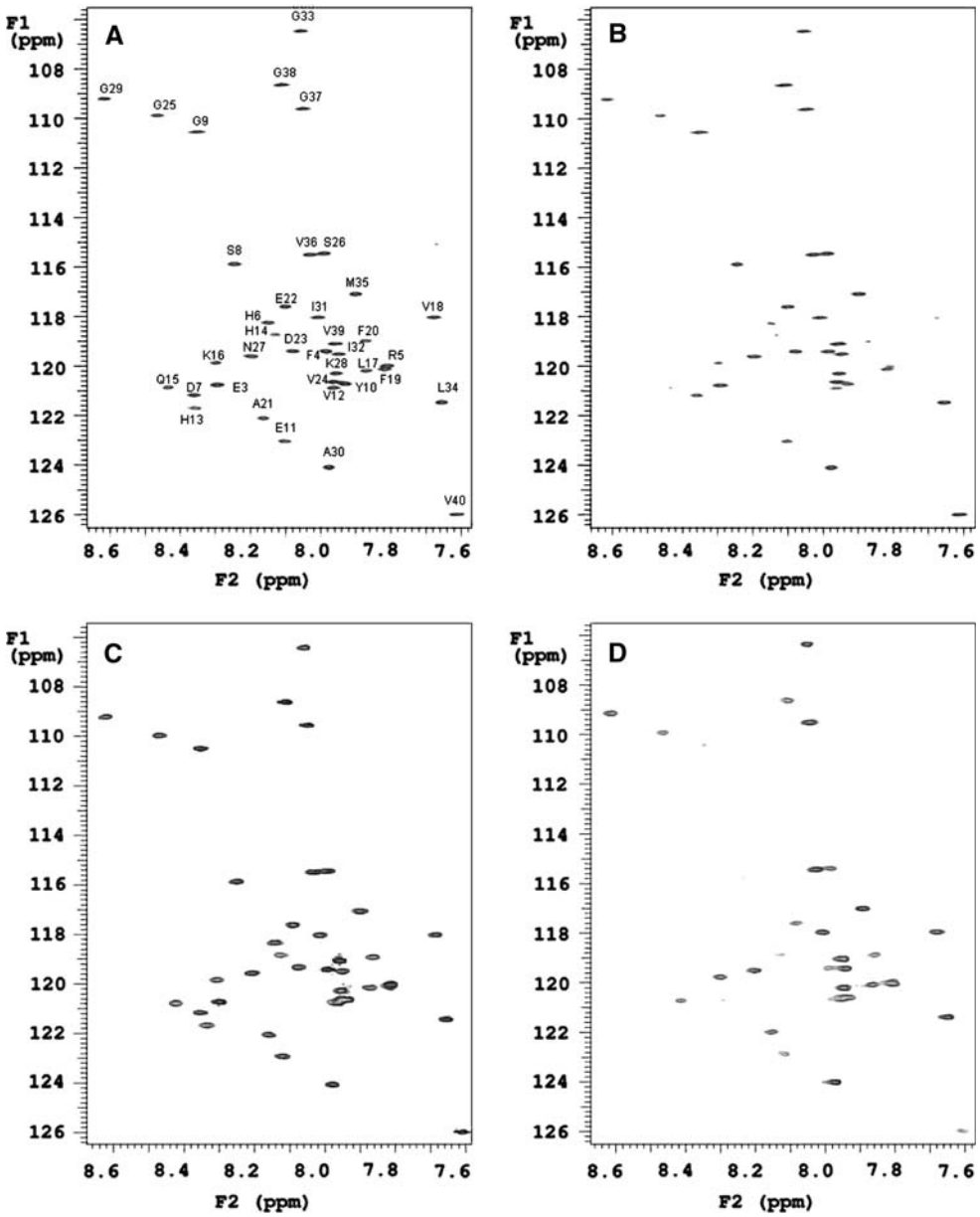

Fig. 1 Effect of paramagnetic agents on Aβ(1–40) spectra in 150 mM SDS-d_{25} at 25°C. 800 MHz ^{1}H–^{15}N TROSY spectra of Aβ(1–40) in SDS at pH 7.3 without (**A**) and with 5-doxyl-stearic acid (**B**). 800 MHz ^{1}H–^{15}N HSQC spectra of ^{15}N labeled Aβ(1–40) (80 μM) at pH 7.4 without (**C**) and with 0.1 mM $MnCl_2$ added (**D**). Cross peaks are labeled using amino acid residue one-letter code

the solvent of the C-terminal helix is also obvious in the TOCSY spectra (data not shown). Figure 3C shows the corresponding data for Aβ(1–40) in an aqueous solvent. In the N-terminus, specific interactions with Mn^{2+} broaden the crosspeaks to a similar degree in both solvents (Fig. 3B and C).

^{15}N relaxation experiments were performed on the Aβ(1–40)/SDS complex in order to determine the effects of the relaxation reagents on the integrity and the size of the micelle (Fig. 2D). The longitudinal relaxation rates were determined both in the presence and absence of Mn^{2+} and 5-doxyl stearic acid. The contribution to the longitudinal relaxation rate from Mn^{2+} is dominated by dipole-dipole relaxation between the magnetic moment of the electron spin and the magnetic moment of the nitrogen spin. As the gyromagnetic ratio of the ^{15}N nuclei is approximately 10-fold smaller than of the protons, the dipole–dipole interaction with electron spins is 10-fold smaller. Relaxation is a second order effect and the contribution to the relaxation rates from the Mn^{2+} ions is approximately 100-fold smaller than the contribution to proton relaxation. Thus, a large effect on the proton relaxation which is monitored by the cross-peak intensities is compatible with a small effect on the ^{15}N-relaxation rates. In the absence of paramagnetic probes the helical region shows relatively constant R_1 values which are generally lower than in the less structured part (Fig. 2D). Addition of Mn^{2+} and 5-doxyl stearic acid does not significantly change the rates

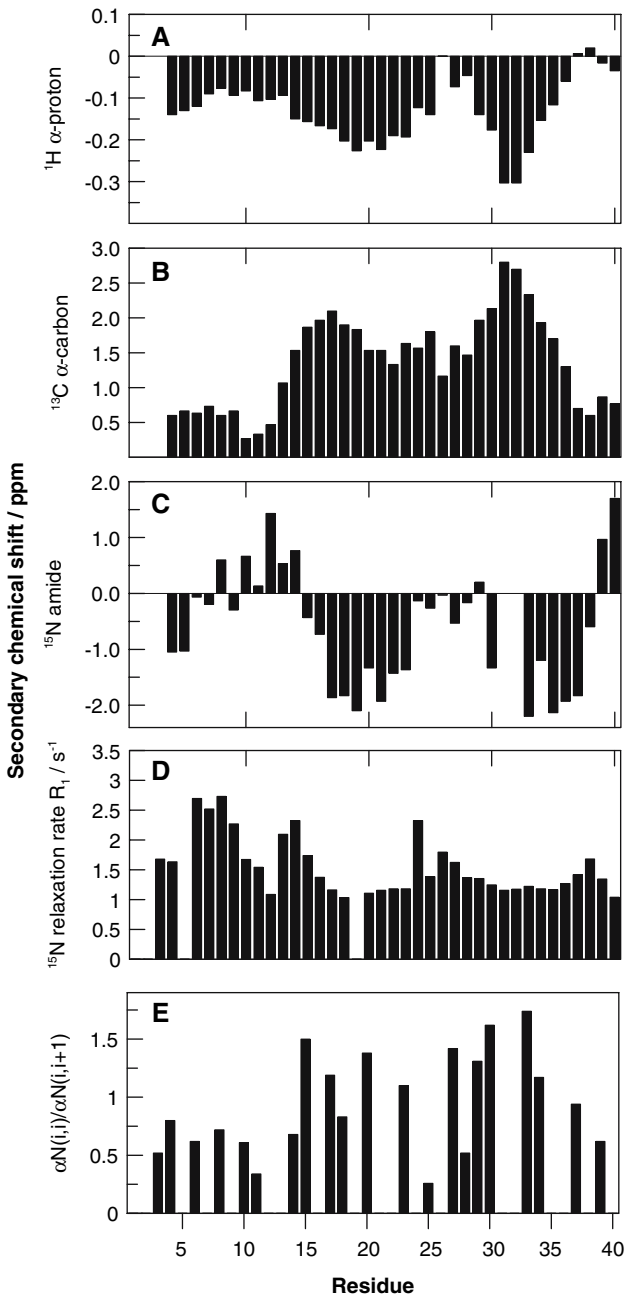

Fig. 2 ^{1}H α-proton, ^{13}C α-carbon, and ^{1}H amide NH secondary chemical shifts. ^{15}N longitudinal relaxation rates R_1 and NOE crosspeak volume ratios $\alpha N(i,i)/\alpha N(i,i+1)$ of Aβ(1–40) in 150 mM SDS-d_{25} at pH 7.4 and 25°C

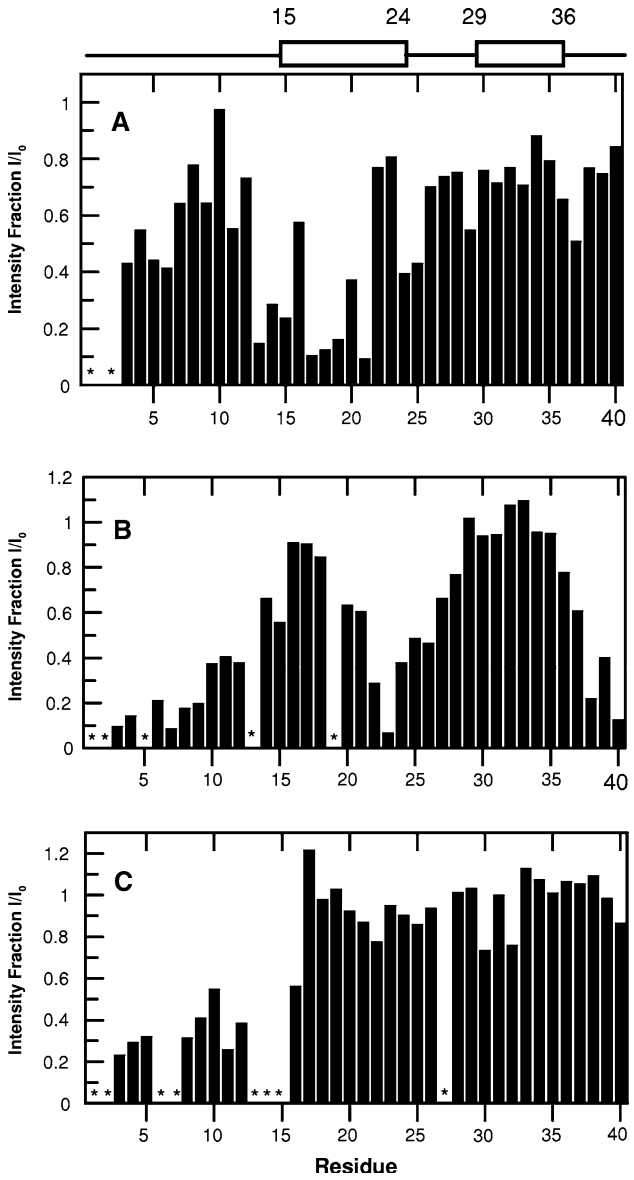

Fig. 3 Comparison of the effects of paramagnetic agents on Aβ(1–40) in 150 mM SDS-d_{25}: 2 mM 5-doxyl stearic acid (**A**), 0.1 mM Mn^{2+} on Aβ(1–40) in the SDS micelles (**B**) and 0.1 mM Mn^{2+} in an aqueous environment, 20 mM phosphate buffer, pH 7.2 and 25°C (**C**). The ratio of integrated crosspeak intensities with and without the paramagnetic agent is plotted along the amino acid sequence. Residues where it was not possible to get reliable intensity ratios because of missing or overlapping crosspeaks are marked with *

(data not shown). This similarity in relaxation rates in absence and presence of the paramagnetic probes shows that the size of the micelle-peptide complex is unchanged upon paramagnetic probe addition.

The faster R_1 relaxation in the more flexible regions of Aβ(1–40) is opposite to the more common situation where very fast (up to tens of picoseconds) internal motions decrease the longitudinal relaxation rates (Papavoine et al. 1997). This pattern is also seen in the free monomeric peptide, where regions with developed secondary structures propensities exhibit slower relaxation rates than the more flexible regions (Danielsson et al. 2006). The increased relaxation rates in the flexible regions show that the internal motions occur on a relatively slow timescale in the approximate range between a few nanoseconds to hundreds of picoseconds. The residues at the outermost termini of Aβ(1–40) in SDS however display somewhat

decreased relaxation rates suggesting a internal motions on a more rapid timescale for these parts of the peptide.

Diffusion experiments

NMR translational diffusion experiments were carried out in order to obtain hydrodynamic information about the peptide/SDS complexes. Diffusion coefficients, determined using the NMR PFG-LED method for Aβ(1–40) in SDS micelles and for SDS micelles at pH 7.6 at 25°C are shown in Table 1. The translational diffusion coefficient for the peptide in SDS solution was compared to diffusion coefficient for the SDS micelle alone and with the free soluble monomeric peptide.

SDS micelle diffusion

In order to determine the diffusion coefficient of the SDS micelle at infinite dilution, the diffusion coefficient of the micelle at different SDS concentrations was determined and analyzed as described in materials and methods. It can be noted that the time to reach equilibrium after diluting the SDS sample is of importance. We found that at least 60 min equilibrium time is necessary to yield stable and reproducible diffusion coefficients. Using this approach to analyze diffusion data from PFG-NMR experiments at 25°C we obtained an SDS micelle self-diffusion coefficient in D_2O, ${}^0D_m = 0.51 \times 10^{-10}$ m^2/s, which corresponds to an unhydrated radius of 28 Å. The radius is obtained by comparing ${}^0D_m$ of SDS with the known ${}^0D_m$ and radius of lysozyme (Chou et al. 2004). In the fit the monomeric diffusion coefficient and critical micelle concentration are not mutually independent and equally good fits may be obtained using different pairs of values on CMC and ${}^0D_f$. Choosing different values of ${}^0D_f$ does not change the fitted values of ${}^0D_m$ and λ, but only alters the CMC value. The value of ${}^0D_f$ may be estimated from the mass of the SDS molecule, using the relation between molecular mass and translational diffusion for unstructured peptides (Danielsson et al. 2002). The monomeric SDS diffusion coefficient at infinite dilution was determined to be ${}^0D_f = 4.8 \times 10^{-10}$ m^2/s. This approach yield a CMC = 6.1 mM, in good agreement with earlier determined values of CMC (Shanks and Franses 1992; Henry and Sykes 1994). The linear relation between micelle concentration and the SDS volume fraction when subtracting the monomer contribution is shown in Fig. 4 and the signal attenuation of the SDS signal and the peptide signal in the NMR diffusion experiment is shown as an insert in Fig. 4. From the slope of the line the parameter λ in Eq. 2 is obtained. For SDS at 25°C λ is close to 1, suggesting that SDS micelles, at these conditions, may be approximated as non-interacting hard spheres. The size of the micelle is also concentration dependent and size increases with increasing concentration (Corti and Degiorgio 1981; Malliaris et al. 1985). This effect is not included in the analysis of diffusion data but that does not change the interpretation of diffusion data in how Aβ binds to and interacts with SDS micelle.

The diffusion coefficient of Aβ(1–40) in the peptide-micelle aggregate shows approximately the same hydrodynamic dimensions as the micelle alone (Table 1). The increase in diffusion coefficient of the peptide-SDS complex compared to the SDS micelle alone is approximately 10%. This corresponds to an equal decrease in hydrodynamic radius. This may arise because the observed peptide diffusion coefficient is the weighted average between free and bound forms of the peptide. The translational diffusion coefficient of the free peptide in D_2O is 1.25×10^{-10} m^2/s (Danielsson et al. 2002) and assuming a fast exchange of the diffusion time scale (100 ms) the bound fraction was determined to be 91%.

Discussion

The positioning of the Aβ(1–40) peptide in the SDS micelles was probed by adding paramagnetic Mn^{2+} ions or 5-doxyl stearic acid to the sample (Damberg et al. 2001b). The overall picture is that both SDS-induced helices are positioned inside the micelle, being less exposed to Mn^{2+}

Table 1 Diffusion coefficients of SDS and Aβ(1–40) incorporated in SDS micelles at 25°C in D_2O

Sample[a]	Diffusion coefficient [10^{-10} m^2/s]	Correction factor for SDS monomer[b]	Correction factor for obstruction[c]	Corrected diffusion coefficient ${}^0D_m$ [10^{-10} m^2/s]	R_H^d [Å]
150 mM SDS	0.59 ± 0.01	0.71	1.2	0.51	28
100 μM Aβ(1–40) in 150 mM SDS	0.48 ± 0.01	1.0[e]	1.2	0.58	

[a] Samples are prepared in 20 mM sodium phosphate buffer at pH 7.2 in D_2O

[b] From Fig. 4: ratio between D_m and D_{obs} at 150 mM SDS concentration

[c] From Fig. 4: ratio between ${}^0D_m$ at 0 mM SDS and D_m at 150 mM SDS concentration

[d] Hydrodynamic radius is determined in relation to the known radius and diffusion coefficient of lysozyme (Chou et al. 2004)

[e] The observed value of Aβ(1–40) diffusion is not influenced by diffusion of SDS monomers

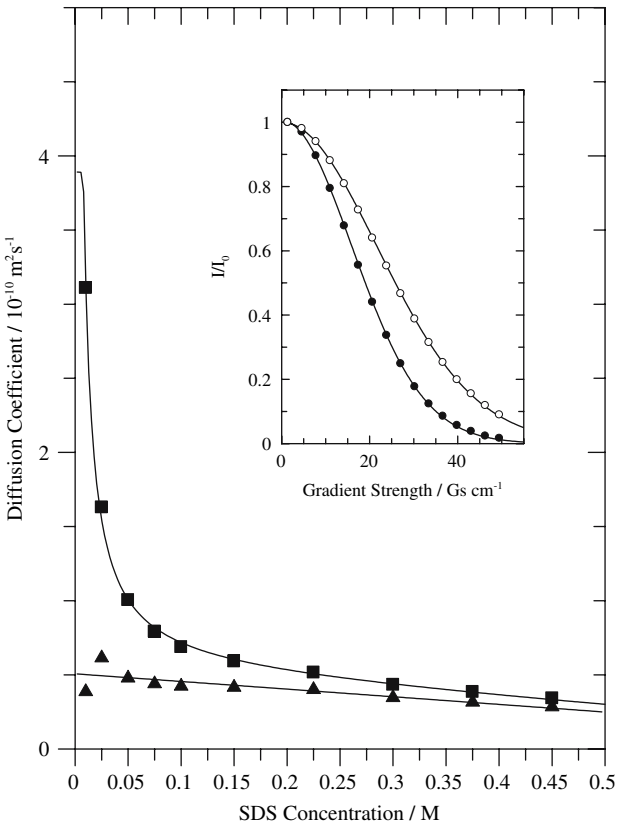

Fig. 4 Concentration dependence of observed diffusion coefficient of SDS. Filled squares are diffusion coefficients, D_{obs}, measured using PFG-NMR including the monomeric contribution to the observed value. Filled triangles are the diffusion coefficient of SDS-micelles, D_m, corrected for the monomeric contribution. The insert shows PFG-NMR attenuation profiles for SDS (filled circles) and Aβ(1–40) (open circles) measured at 150 mM concentration. The apparent difference in the diffusion coefficients between the peptide and SDS micelles is due to the presence of monomeric SDS

in the solvent than the other regions. As suggested from the interactions with 5-doxyl stearic acid, the central helix (residues 15–24) should lie close to the headgroup layer, with the face composed of residues 16, 20 and 22, 23 facing the external medium. This suggests an amphipathic nature of this helix. The C-terminal helix, residues 29–35) is more deeply buried in the interior of the micelle. The unstructured, more flexible parts of the peptide are clearly in closer contact with the Mn^{2+} in the solvent, and should therefore be positioned at or outside the surface of the micelle.

In a pure aqueous solution with a low concentration of Mn^{2+} (Fig. 3C), this ion seems to be specifically bound to ligands in the N-terminus of Aβ(1–40), similar to what has been shown for Cu^{2+} and Zn^{2+} ions (Syme et al. 2004; Danielsson et al. 2007). Copper and zinc ions bind specifically to the three histidines in the N-terminal part of the peptide and the fourth ligand is the N-terminal aspartic acid. Our results from the pure aqueous solution suggest the Mn^{2+} shares the same binding site and binding mode as copper and zinc. Therefore resonances from residues 1–15 are strongly broadened in aqueous solution, whereas those from residues 16–40 are less affected. By comparing Fig. 3B and C, it is possible to conclude that the N-terminus also in the SDS solvent is similarly and strongly affected, supporting the interpretation that the N-terminus of Aβ(1–40) is at or outside the headgroup layer of the SDS micelle.

Longitudinal relaxation rates for amide ^{15}N shows that the helices are more rigid than the N-terminal part of the peptide. In addition, the region between the helices has a higher mobility than the helices. This pattern is present also in the unstructured monomeric peptide in water solution, suggesting that the propensity for Aβ to adopt an α-helical secondary structure is SDS is reflected in the dynamical properties of the peptide in aqueous solution (Danielsson et al. 2006).

In the present study we could determine whether the peptide/SDS interaction affects the size of the SDS micelle. By measuring the translational diffusion coefficient of the peptide/micelle complex by NMR we have estimated the hydrodynamic properties and size of the complex. Our data suggests that the peptide/micelle complex has approximately the same size as the SDS micelle alone. Another important piece of information from the diffusion data is that it is possible to estimate the bound and free fractions of the peptide. In this system the bound peptide fraction is 91% and this small amount is not expected to influence the positioning determination significantly.

The SDS micelle is small and the surface is highly charged. By electrostatic attraction we would expect the Mn^{2+} concentration to be high in the headgroup layer of the micelle. Copper has been shown to colocalize with Aβ and SDS/water interface (Lau et al. 2006), and this is the likely place for the local interactions leading to signal broadening. The C-terminal helix is the most hydrophobic one of the two induced helices. It is not unexpected that this helix is inserted into the hydrophobic interior of the micelle.

Using the paramagnetic relaxation enhancement data, together with the structural and hydrodynamic data leads to a course grain model of the Aβ(1–40) in complex with the SDS micelle. Figure 5 gives a cartoon model of the peptide/SDS complex. Our model of Aβ(1–40) in complex with the SDS-model supports one of the hypothetic positioning models suggested by Craik and coworkers (model A, Fig. 11 in Coles et al. 1998). It is also similar to one building-block of the hypothetic architecture of an Aβ membrane channel (Durell et al. 1994; Arispe et al. 2004). The Aβ peptide positioning in a membrane-mimicking environment as experimentally determined in the present study is an important issue, because of the potential

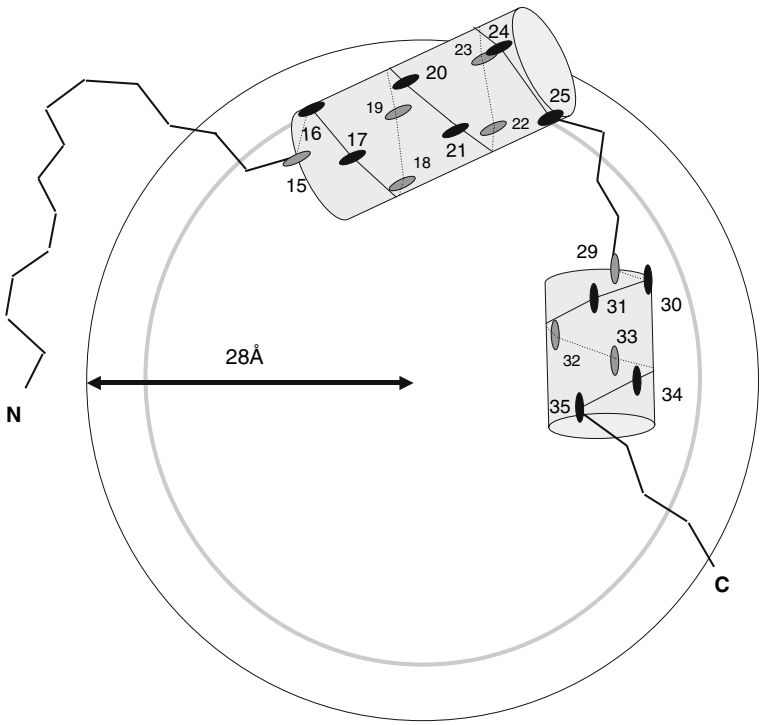

Fig. 5 Model for Aβ(1–40) interaction with an SDS micelle. The two α-helices involve residues 15–24 and 29–35. The inner gray circle shows approximately the inner limit of the region affected by 5-doxyl stearic acid. The micelle diameter was estimated from the translational diffusion measurements taking into the account the presence of monomeric SDS

formation of membrane channels which are suggested to be responsible for the neurotoxic activity of the peptide.

Acknowledgements We wish to thank Karolina Åseby for help with the initial experiments and Evangelos Papadopoulos for help with the sparky program. The Swedish NMR centre is acknowledged for the use of the 800 MHz NMR spectrometer. This work was supported by grant from the Swedish Research Council, the Lars Hierta Foundation and by the European Commission, contract LSHG-CT-2004-512051.

References

Alarcón JM, Brito JA, Hermosilla T, Atwater I, Mears D, Rojas E (2006) Ion channel formation by Alzheimer's disease amyloid β-peptide (Aβ40) in unilamellar liposomes is determined by anionic phospholipids. Peptides 27:95–104

Ambroggio EE, Kim DH, Separovic F, Barrow CJ, Barnham KJ, Bagatolli LA, Fidelio GD (2005) Surface behavior and lipid interaction of Alzheimer β-amyloid peptide 1–42: a membrane-disrupting peptide. Biophys J 88: 2706–2713

Arispe N (2004) Architecture of the Alzheimer's AβP ion channel pore. J Membr Biol 197:33–48

Ashley RH, Harroun TA, Hauss T, Breen KC, Bradshaw JP (2006) Autoinsertion of soluble oligomers of Alzheimer's Aβ(1–42) peptide into cholesterol-containing membranes is accompanied by relocation of the sterol towards the bilayer surface. BMC Struct Biol 6:21

Barghorn S, Nimmrich V, Striebinger A, Krantz C, Keller P, Janson B, Bahr M, Schmidt M, Bitner RS, Harlan J, Barlow E, Ebert U, Hillen H (2005) Globular amyloid β-peptide1–42 oligomer — a homogenous and stable neuropathological protein in Alzheimer's disease. J Neurochem 95:834–847

Bokvist M, Lindström F, Watts A, Gröbner G (2004) Two types of Alzheimer's β-amyloid(1–40) peptide membrane interactions: aggregation preventing transmembrane anchoring versus accelerated surface fibril formation. J Mol Biol 335:1039–1049

Chiti F, Dobson CM (2006) Protein misfolding, functional amyloid, and human disease. Annu Rev Biochem 75:333–366

Chou JJ, Baber JL, Bax A (2004) Characterization of phospholipid mixed micelles by translational diffusion. J Biomol NMR 29:299–308

Coles M, Bicknell W, Watson AA, Fairlie DP, Craik DJ (1998) Solution structure of amyloid β-peptide(1–40) in a water-micelle environment. Is the membrane-spanning domain where we think it is? Biochemistry 37:11064–11077

Corti M, Degiorgio V (1981) Quasi-elastic light scattering study of intermicellar interactions in aqueous sodium dodecyl sulfate solutions. J Phys Chem 85:711–717

Crescenzi O, Tomaselli S, Guerrini R, Salvadori S, D'Ursi AM, Temussi PA, Picone D (2002) Solution structure of the Alzheimer amyloid β-peptide(1–42) in an apolar microenvironment. Similarity with a virus fusion domain. Eur J Biochem 269:5642–5648

Curtain CC, Ali F, Volitakis I, Cherny RA, Norton RS, Beyreuther K, Barrow CJ, Masters CL, Bush AI, Barnham KJ (2001) Alzheimer's disease amyloid-β binds copper and zinc to generate an allosterically ordered membrane-penetrating structure containing superoxide dismutase-like subunits. J Biol Chem 276:20466–20473

Damberg P, Jarvet J, Gräslund A (2001a) Accurate measurement of translational diffusion coefficients: a practical method to account for nonlinear gradients. J Magn Reson 148:343–348

Damberg P, Jarvet J, Gräslund A (2001b) Micellar systems as solvents in peptide and protein structure determination. Methods Enzymol 339:271–285

Danielsson J, Andersson A, Jarvet J, Gräslund A (2006) ^{15}N relaxation study of the amyloid β-peptide: structural propensities and persistence length. Magn Reson Chem 44:S114–S121

Danielsson J, Jarvet J, Damberg P, Gräslund A (2002) Translational diffusion measured by PFG-NMR on full length and fragments of the Alzheimer Aβ(1–40) peptide. Determination of hydrodynamic radii of random coil peptides of varying length. Magn Reson Chem 40:S89–S97

Danielsson J, Pierattelli R, Banci L, Gräslund A (2007) High-resolution NMR studies of the zinc-binding site of the Alzheimer's amyloid β-peptide. FEBS J 274:46–59

Demuro A, Mina E, Kayed R, Milton SC, Parker I, Glabe CG (2005) Calcium dysregulation and membrane disruption as a ubiquitous neurotoxic mechanism of soluble amyloid oligomers. J Biol Chem 280:17294–17300

Durell SR, Guy HR, Arispe N, Rojas E, Pollard HB (1994) Theoretical models of the ion channel structure of amyloid β-protein. Biophys J 67:2137–2145

Ege C, Lee KY (2004) Insertion of Alzheimer's Aβ40 peptide into lipid monolayers. Biophys J 87:1732–1740

Fletcher TG, Keire DA (1997) The interaction of β-amyloid protein fragment (12–28) with lipid environments. Protein Sci 6:666–675

Gibbs SJ, Morris KF, Johnson CS (1991) Design and implementation of a shielded gradient coil for PFG NMR diffusion and flow studies. J Magn Reson 94:165–169

Hardy J, Selkoe DJ (2002) The amyloid hypothesis of Alzheimer's disease: progress and problems on the road to therapeutics. Science 297:353–356

Henry GD, Sykes BD (1994) Methods to study membrane protein structure in solution. Methods Enzymol 239:515–535

Ji SR, Wu Y, Sui SF (2002) Cholesterol is an important factor affecting the membrane insertion of β-amyloid peptide (Aβ1–40), which may potentially inhibit the fibril formation. J Biol Chem 277:6273–6279

Johannesson H, Halle B (1996) Solvent diffusion in ordered macrofluids: a stochastic simulation study of the obstruction effect. J Chem Phys 104:6807–6817

Kayed R, Head E, Thompson JL, McIntire TM, Milton SC, Cotman CW, Glabe CG (2003) Common structure of soluble amyloid oligomers implies common mechanism of pathogenesis. Science 300:486–489

Kayed R, Sokolov Y, Edmonds B, McIntire TM, Milton SC, Hall JE, Glabe CG (2004) Permeabilization of lipid bilayers is a common conformation-dependent activity of soluble amyloid oligomers in protein misfolding diseases. J Biol Chem 279:46363–46366

Klein WL, Krafft GA, Finch CE (2001) Targeting small Aβ oligomers: the solution to an Alzheimer's disease conundrum? Trends Neurosci 24:219–224

Kupče Ē, Freeman R (1995) Adiabatic pulses for wideband inversion and broadband decoupling. J Magn Reson 115A:273–276

Kohno T, Kobayashi K, Maeda T, Sato K, Takashima A (1996) Three-dimensional structures of the amyloid β peptide (25–35) in membrane-mimicking environment. Biochemistry 35:16094–16104

Lacor PN, Buniel MC, Chang L, Fernandez SJ, Gong Y, Viola KL, Lambert MP, Velasco PT, Bigio EH, Finch CE, Krafft GA, Klein WL (2004) Synaptic targeting by Alzheimer's-related amyloid β oligomers. J Neurosci 24:10191–10200

Lau TL, Ambroggio EE, Tew DJ, Cappai R, Masters CL, Fidelio GD, Barnham KJ, Separovic F (2006) Amyloid-β peptide disruption of lipid membranes and the effect of metal ions. J Mol Biol 356:759–770

Lee JP, Stimson ER, Ghilardi JR, Mantyh PW, Lu YA, Felix AM, Llanos W, Behbin A, Cummings M, Van Criekinge M (1995) ^{1}H NMR of Aβ amyloid peptide congeners in water solution. Conformational changes correlate with plaque competence. Biochemistry 34:5191–5200

Lesné S, Koh MT, Kotilinek L, Kayed R, Glabe CG, Yang A, Gallagher M, Ashe KH (2006) A specific amyloid-β protein assembly in the brain impairs memory. Nature 440:352–357

Lin H, Bhatia R, Lal R (2001) Amyloid β protein forms ion channels: implications for Alzheimer's disease pathophysiology. FASEB J 15:2433–2444

Malliaris A, Moigne JL, Sturm J, Zana R (1985) Temperature dependence of the micelle aggregation number and rate of intramicellar excimer formation in aqueous surfactant solutions. J Phys Chem 89:2709–2713

Mandal PK, Pettegrew JW, McKeag DW, Mandal R (2006) Alzheimer's disease: halothane induces Aβ peptide to oligomeric form—solution NMR studies. Neurochem Res 31:883–890

Mandal PK, Williams JP, Mandal R (2007) Molecular understanding of Aβ peptide interaction with isoflurane, propofol, and thiopental: NMR spectroscopic study. Biochemistry 46:762–771

Micelli S, Meleleo D, Picciarelli V, Gallucci E (2004) Effect of sterols on β-amyloid peptide (AβP 1–40) channel formation and their properties in planar lipid membranes. Biophys J 86: 2231–2237

Papavoine CH, Remerowski ML, Horstink LM, Konings RN, Hilbers CW, van de Ven FJ (1997) Backbone dynamics of the major coat protein of bacteriophage M13 in detergent micelles by ^{15}N nuclear magnetic resonance relaxation measurements using the model-free approach and reduced spectral density mapping. Biochemistry 36:4015–4026

Quist A, Doudevski I, Lin H, Azimova R, Ng D, Frangione B, Kagan B, Ghiso J, Lal R (2005) Amyloid ion channels: a common structural link for protein-misfolding disease. Proc Natl Acad Sci USA 102:10427–10432

Sokolov Y, Kozak JA, Kayed R, Chanturiya A, Glabe C, Hall JE (2006) Soluble amyloid oligomers increase bilayer conductance by altering dielectric structure. J Gen Physiol 128:634–637

Selkoe DJ (2003) Folding proteins in fatal ways. Nature 426:900–904

Shao H, Jao S, Ma K, Zagorski MG (1999) Solution structures of micelle-bound amyloid β-(1–40) and β-(1–42) peptides of Alzheimer's disease. J Mol Biol 285:755–773

Shanks PC, Franses EI (1992) Estimation of micellization parameters of aqueous sodium dodecyl sulfate from conductivity data. J Phys Chem 96:1794–1805

Sticht H, Bayer P, Willbold D, Dames S, Hilbich C, Beyreuther K, Frank RW, Rösch P (1995) Structure of amyloid A4-(1–40)-peptide of Alzheimer's disease. Eur J Biochem 233:293–298

Syme CD, Nadal RC, Rigby SE, Viles JH (2004) Copper binding to the amyloid-β (Aβ) peptide associated with Alzheimer's disease: folding, coordination geometry, pH dependence, stoichiometry, and affinity of Aβ-(1–28): insights from a range of complementary spectroscopic techniques. J Biol Chem 279:18169–18177

Talafous J, Marcinowski KJ, Klopman G, Zagorski MG (1994) Solution structure of residues 1–28 of the amyloid β-peptide. Biochemistry 33:7788–7796

Terzi E, Hölzemann G, Seelig J (1994) Alzheimer β-amyloid peptide 25–35: electrostatic interactions with phospholipid membranes. Biochemistry 33:7434–7441

Tokuyama M, Oppenheim I (1994) Dynamics of hard-sphere suspensions. Phys Rev E Stat Phys Plasmas Fluids Relat Interdiscip Topics 50:R16–R19

Wishart DS, Bigam CG, Yao J, Abildgaard F, Dyson HJ, Oldfield E, Markley JL, Sykes BD (1995) ^{1}H, ^{13}C and ^{15}N chemical shift referencing in biomolecular NMR. J Biomol NMR 6:135–140